Appl. Phys. B 79, 485–489 (2004)
DOI: 10.1007/s00340-004-1600-9

Applied Physics B
Lasers and Optics

J.A. SWANSSON[1]
K.G.H. BALDWIN[1,2,✉]
M.D. HOOGERLAND[3]
A.G. TRUSCOTT[1,2]
S.J. BUCKMAN[1]

A high flux, liquid-helium cooled source of metastable rare gas atoms

[1] Research School of Physical Sciences and Engineering, The Australian National University, Canberra, ACT 0200, Australia
[2] Australian Research Council Centre of Excellence for Quantum-Atom Optics, Australia
[3] Department of Physics, University of Auckland, Private Bag 92019, Auckland, New Zealand

Received: 19 January 2004/Revised version: 5 May 2004
Published online: 22 July 2004 •

ABSTRACT We have developed a novel, high flux source of metastable rare gas atoms (helium, neon and argon) that uses liquid helium cooling to reduce the initial atomic velocity. Fluxes exceeding 10^{14} atoms/ster/s with He and Ne were obtained. With average velocities of ~ 600 m/s for He and ~ 300 m/s for Ne and Ar, this source will enable simpler, more compact beam lines for loading magneto-optical traps.

PACS 34.80.Dp; 39.10.+j; 39.25.+k

1 Introduction

High flux sources of metastable rare gas atoms are important for a range of applications in atom optics and atomic physics [1, 2]. In particular, high flux sources are important for the efficient loading of magneto-optic traps (MOTs), which are the workhorse for many experiments including the preparation of atoms for Bose–Einstein condensation (BEC) [3]. A further requirement for efficient MOT-loading sources is that a significant fraction of the atomic velocity distribution should be within the velocity capture range of the MOT (typically < 100 m/s [4]) in order to facilitate rapid loading. This can be achieved by a combination of cryogenic cooling of the metastable atomic source, and laser cooling/focusing of the resulting atomic beam [2, 5].

In a previous paper we reported on the development of a liquid-nitrogen cooled metastable helium source [1] which yielded high fluxes (up to 10^{15} atoms/ster/s) with average velocities ~ 1000 m/s. This source is used directly in applications such as atom lithography [6], or as an input to our bright metastable helium beam line [5] which slows the metastable He atoms to < 100 m/s. The bright beam line is used for applications such as atom guiding in hollow optical fibres [7], and for loading a metastable He MOT [8].

However, the bright beam line requires a Zeeman slower over two metres in length, which in turn requires transverse collimation and finally focusing to maintain a high beam brightness. It would be desirable to use liquid-helium cooling of the source to reduce the initial beam velocity and, in turn, reduce the length and complexity of the beam line for MOT loading. Such a source has been developed elsewhere [2] with average velocities of ~ 300 m/s, but with relatively low flux ($< 10^{13}$ atoms/ster/s). Here we investigate a new type of liquid-He cooled metastable source that generates higher fluxes more comparable with our liquid-N_2 cooled source.

✉ Fax: +61-2/6125-2452, E-mail: Kenneth.Baldwin@anu.edu.au

2 Source design

Conventional metastable rare gas discharge sources typically employ a sharp needle cathode inside a gas reservoir, and an exit nozzle to allow gas expansion into a vacuum chamber [9–11]. In order to prevent metastable density loss arising from inter-atomic collisions during the expansion, an external anode is employed to create a discharge through the nozzle into the collision-free region located many nozzle diameters downstream [1, 12]. This requires high source pressures and currents to sustain the discharge, which consequently increases the discharge temperature and hence the atomic velocity. For this reason, the nozzle was used as the anode in reference [2]. This source was operated at low pressures ($\sim 10^{-2}$ mbar) to avoid collision losses, significantly limiting the maximum achievable flux.

In the present experiments, we aim for a high flux source with similar output to our previous source but with reduced velocity through liquid-He cooling. To increase the number of atoms in the low-velocity tail of the atomic velocity distribution, it is often desirable to operate the source closer to the effusive [13] rather than the supersonic [14] regime. The velocity distributions in Fig. 1 illustrate the implications for design. The implications of the data are discussed later in Sect. 4.

The velocity distribution is given by [14]:

$$P(v) \propto v^3 \exp\left[-\frac{m(v-u(M))^2}{v_{\mathrm{th}}^2(M)}\right], \qquad (1)$$

where $u(M)$ is the average (flow) velocity, and corresponds to the velocity of the peak, and $v_{\mathrm{th}}(M)$ the local thermal velocity, which determines the width of the distribution. Both vary as a function of the final Mach number M.

Operation closer to the effusive regime requires larger nozzle diameters and/or lower operating pressures. However, a needle cathode discharge cannot be sustained at pressures much below 30 mbar. Consequently, we embarked upon a new design based on a hollow cathode whose larger surface area

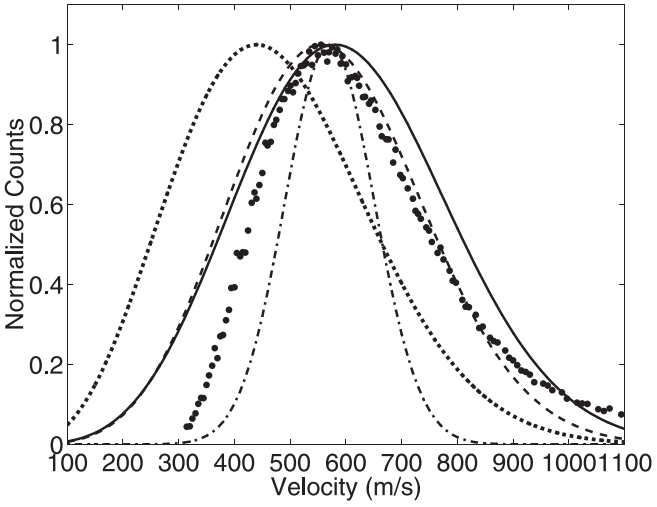

FIGURE 1 Effusive (*dotted*) and supersonic ($M = 1$, *dashes*; $M = 3$, *solid*; $M = 5$, *dash-dot*) velocity distributions for a source temperature of ~ 25 K as a function of Mach number. The data points are taken using the final version of the hollow cathode at a pressure of 0.36 Torr and 400 volts

is capable of operation at lower discharge pressures. The increased area maintains a higher current for a given discharge voltage, and hence a lower turn-on voltage and lower power consumption are possible to reduce heating.

A number of hollow cathode sources were tested to determine the optimum configuration, and these are illustrated in Fig. 2. The source is constructed from a hollowed copper block – the hollow cathode – with varying nozzle/anode configurations. An insulating collar made of boron nitride guarantees a region for positive column plasma in configurations A–C.

In configurations A and B the nozzle plate is metallic (copper) and acts as the anode. The nozzle is shaped to achieve the sharpest curvature at the outer surface in order to initiate the discharge at this point and maximize the excitation of atoms travelling through the nozzle itself. Configuration B insulates the majority of the interior anode surface away from the nozzle by using a boron nitride washer as a shield. This concentrates the discharge around the nozzle and hence increases the number of electron-atom collisions in the region of the nozzle.

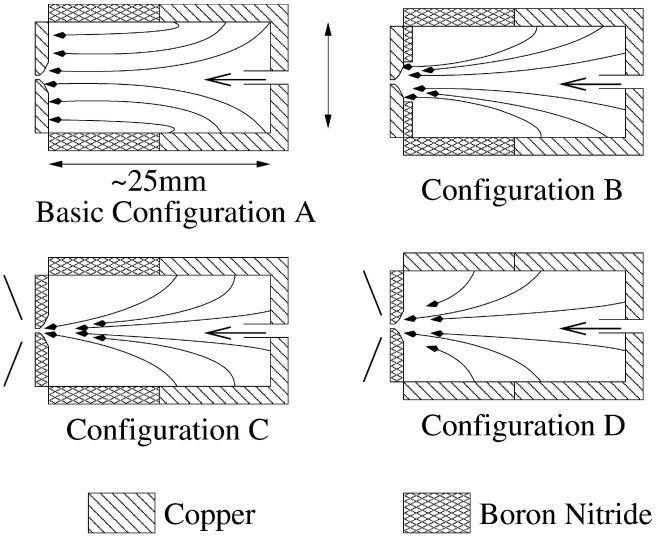

FIGURE 2 Hollow cathode discharge source with four design configurations. Gas inlet – *large arrow*, *right*; nozzle – *left*; *other arrows* indicate the discharge path. C and D have external anodes

Configurations C and D use an insulator (boron nitride) as the nozzle plate, with an external anode formed by an aluminium cone just outside the nozzle. This design intends to compensate for the collisional losses within the nozzle itself by maintaining a region of metastable excitation just external to the nozzle (as used in our previous source [1]). Configuration D removes the internal insulating boron nitride collar, to maximise the cathode surface area available for the discharge current.

3 Experimental description

The source block is mounted on a Janis continuous-flow liquid-He cryostat (model ST-100), which could be cooled to a temperature of ~ 5 K, measured using a silicon detector. Tests indicate that the cryostat can maintain this temperature with minimal liquid-He flow for power inputs up to 2 W. A layer of indium foil is mounted between the source block and the cold-finger to improve surface contact and heat dissipation.

Consequently the hollow cathode is grounded permanently. This has the added advantage of obviating precautions against discharge breakdown leakage (as required for our liquid-N_2 cooled source [1]) as well as allowing operation using a single power supply. The discharge voltage applied to the anode can be as low as 300 V at higher pressures (~ 0.5 Torr) and temperatures (~ 70 K). The discharge spontaneously starts at 400–600 V at these conditions, but can be started using a short 5 kV pulse at lower temperatures and pressures.

The source chamber is pumped by a 1400 l/s turbo-pump (Balzers–Pfeiffer TMU1601). The background helium pressure during operation is 10^{-5}–10^{-4} Torr at typical source pressures of 0.1–1.0 Torr. Consequently, losses due to collisions in the source chamber are negligible. The metastable beam then passes through a skimmer, located 5–10 mm from the nozzle, into the differentially-pumped beamline which is maintained at a pressure of $< 10^{-6}$ Torr.

Immediately after the skimmer are several components to condition and characterize the atomic beam, Fig. 3. First the beam passes through a glass-coil He discharge tube. The light from this discharge quenches any atoms in the $2\,^1S_0$ singlet metastable state. Charged particles in the beam are removed by an electric potential between two parallel plates set at ± 200 V. Nitrogen can be fed into the beamline chamber via a bleed valve to collisionally quench the metastable atoms. A rotating wire detector can be moved into place to measure the local beam current at a range of positions in the atomic beam. The total beam current is measured by inserting a 40 mm diameter, 50% transmission stainless steel grid (not shown).

For time-of-flight velocity measurements, the atomic beam is chopped using an in-vacuo mechanical chopper. A 100 mm wheel with a 1 mm slot rotates at ~ 60 Hz.

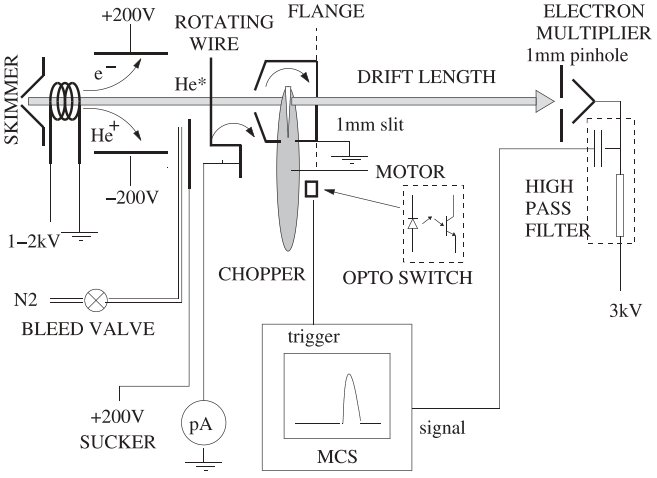

FIGURE 3 Experimental apparatus, showing beam conditioning devices and detectors, with time-of-flight system at right. The opto-switch operated across the chopper slit provides the timing trigger for the TOF signal

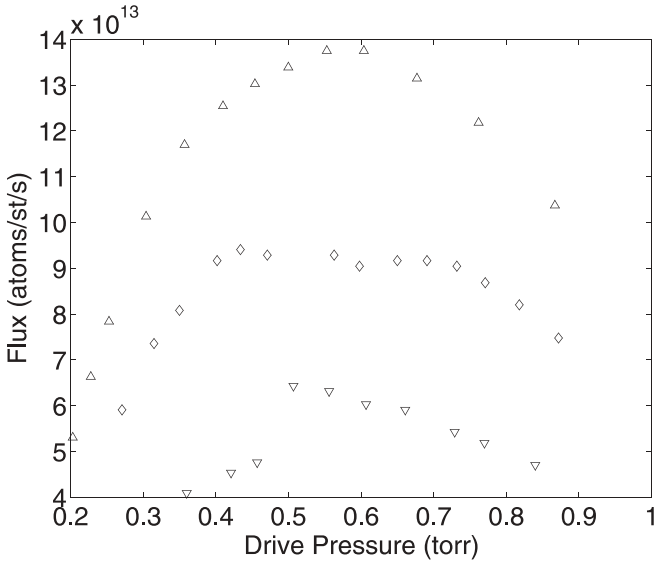

FIGURE 4 Atomic flux as a function of drive pressure for source voltages: 600 V (▽); 1000 V(◇); and 1500 V (△). Note that there is a discharge mode change at ∼ 0.45 Torr, especially for lower discharge voltages

Both UV photons and metastable atoms in the $2\,^3S_1$ triplet metastable state emitted from the source are detected after the 1120 mm drift distance L_{TOF} by an ETP electron multiplier. To control the detected flux, improve the temporal resolution and reduce stray UV light reflections, the atomic beam is collimated by a 1 mm fixed slot at the chopper wheel and a 1 mm pinhole at the detector. The electron multiplier signal is collected by a multi-channel scaler (MCS) which is triggered by an opto-reflective switch aligned with a hole in the chopper wheel.

4 Results

The atomic flux from all four source configurations showed a similar dependence on the discharge current and on the source pressure. As for the liquid-N_2 cooled source [1], the flux was linear with the discharge current. The flux increases with drive pressure to a maximum at ∼ 0.5 Torr, at which pressure the metastable flux is limited by quenching collisions, Fig. 4. Under typical operating conditions, with the ion contribution removed from the beam, photons typically comprise ∼ 20% of the total beam flux, and singlet ($^1S_0$) metastables ∼ 10% of the total flux. The transverse profile of the beam is measured with the rotating wire, and has a typical full width at half maximum (FWHM) of ∼ 40 mm approximately 260 mm downstream from the skimmer.

The TOF spectra exhibited two signal peaks: an instantaneous peak due to UV photons from the discharge, and the $2\,^3S_1$ atom peak following the drift time. The photon peak is used to determine the zero of the time scale t_0, and the TOF distribution $I(t)$ is given by [15]

$$I(t) \propto \left(\frac{L_{\mathrm{TOF}}}{t v_{\mathrm{th}}}\right)^5 \exp\left[-\left(\frac{L_{\mathrm{TOF}}}{t v_{\mathrm{th}}} - \frac{u}{v_{\mathrm{th}}}\right)^2\right]. \qquad (2)$$

Using the transformations

$$v = L_{\mathrm{TOF}}/(t - t_0) \text{ and}$$
$$P(v)\,\mathrm{d}v = (L_{\mathrm{TOF}}/t^2) I(t)\,\mathrm{d}t$$

yields the experimental velocity distribution, which can in turn be compared to the theoretical velocity distribution given by (1). Deconvolution of the TOF instrument function (represented by the light peak) was not necessary because the light peak was significantly narrower than the He* time-of-flight signal, and because we use the average velocity simply as a general indicator of the performance of the source.

Inspection of Fig. 1 indicates that the best source velocity distribution is supersonic, rather than effusive. The experimental data best fits the peak location and width with a Mach number of ∼ 3. The missing counts in the low velocity edge are attributed to the higher interaction times and susceptibility to quenching and trajectory altering collisions. The velocity ranges and atomic flux are shown for the various source configurations in Fig. 5. Note that at the measured cryostat cold-finger temperature during source operation (5 K), the average velocity for an effusive molecular beam is

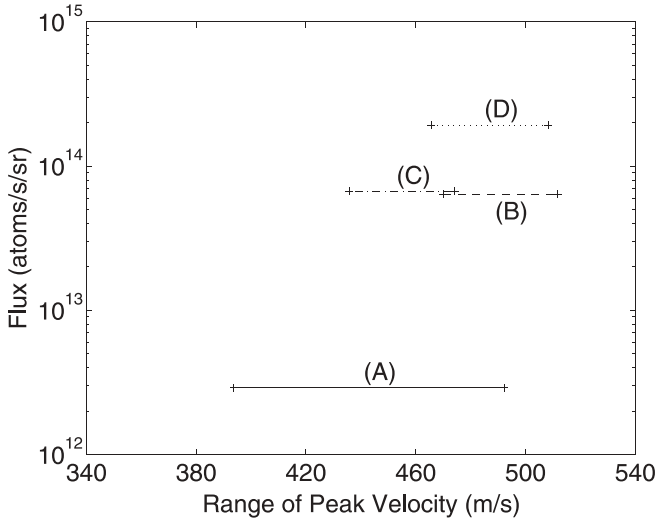

FIGURE 5 Atomic flux and velocity ranges (∝ drive pressure) for the four source versions in Fig. 2, at minimum operating voltages

$1.33\alpha \sim 200$ m/s [13] where

$$\alpha = \sqrt{2kT/m} \tag{3}$$

and k is Boltzmann's constant with m the mass of the atom. The fact that the measured average velocities are significantly higher is a combination of the discharge temperature being higher than the surrounding environment, and the source operating in the supersonic regime.

There is little difference in average velocity between the source configurations operating under similar conditions. As expected, the external anode sources (configurations C and D) yield higher fluxes as a result of the discharge being present well into the collision-free region. The highest flux is produced by the external anode source without the insulating collar (configuration D) for which there was only a small increase in average velocity. Consequently, this configuration was adopted for subsequent investigations.

To determine whether the source could be operated closer to the effusive regime, the average velocity was measured as a function of source pressure. Figure 6 shows a reduction in average velocity to just over 450 m/s at the lowest pressures at various discharge currents. The lower pressures resulted in a significant reduction in flux, so a compromise operating condition of 300–350 mTorr and 400–600 volts was typically employed.

The average velocity can also be reduced by increasing the nozzle diameter and operating closer to effusive source conditions, while at the same time increasing the flux. Figure 7 illustrates the effect of nozzle size on the beam flux at the operating conditions above. Both the highest flux and the lowest velocity were obtained for a 1.0 mm nozzle diameter, which was adopted as the optimum source configuration. The decrease in flux for the largest nozzle size may be the result of quenching collisions in the source chamber due to the higher background pressure. The data also clearly show the supersonic effect of higher velocities from the narrower nozzle. The maximum flux (exceeding 10^{14} atoms/ster/s) is an order of magnitude less

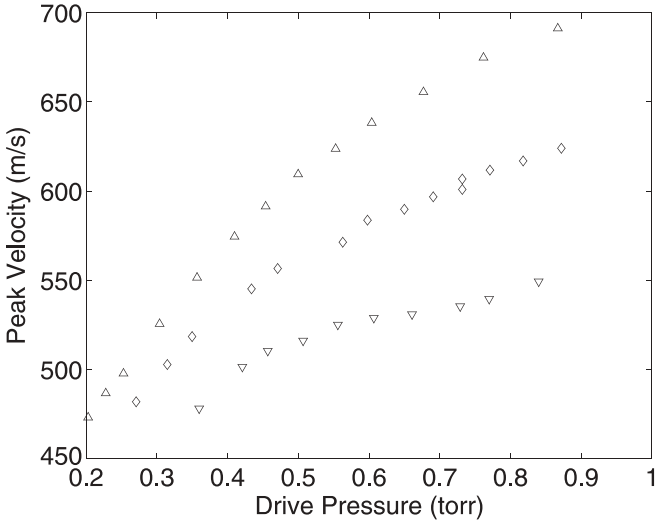

FIGURE 6 Peak velocity, for source D, as a function of drive pressure for source currents: 2.7 mA (▽); 5.0 mA (◇); and 8.2 mA (△)

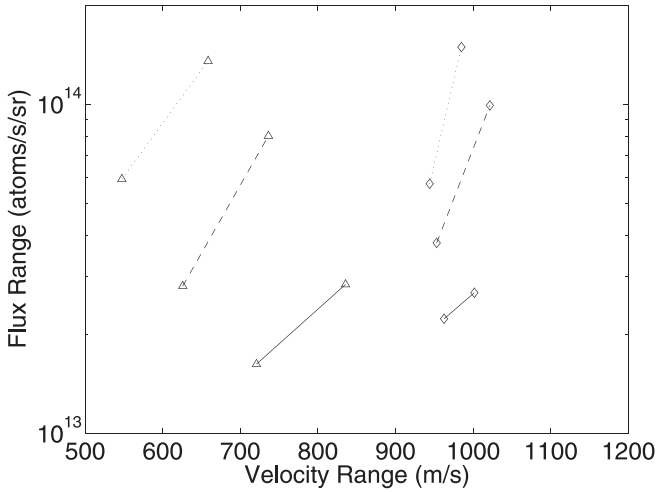

FIGURE 7 Range of beam flux vs velocity for liquid He (△) and N_2 (◇) cooling for nozzle diameters: 0.5 mm – *solid*; 1.0 mm – *dots*; 1.2 mm – *dashes*

than our previous liquid-N_2 cooled source [1] but the average velocity is reduced by a factor of two. A greater velocity reduction might be expected given the relative temperatures of liquid helium and nitrogen, so we conclude that the discharge temperature has a greater influence on the velocity distribution of the liquid helium-cooled, He* source.

The continuous flow cryostat could be operated using liquid N_2, and Fig. 7 shows the flux and velocity obtained at these temperatures. Once again the 1.0 mm nozzle yielded the best performance with a velocity (~ 1000 m/s) comparable to our liquid-N_2 cooled source reported previously [1] and a flux exceeding 10^{14} atoms/ster/s.

Since the cryostat is capable of operating at a fixed temperature (monitored by the silicon detector and adjusted using a heating element), the source can be used to generate a range of metastable atomic species when operated just above their

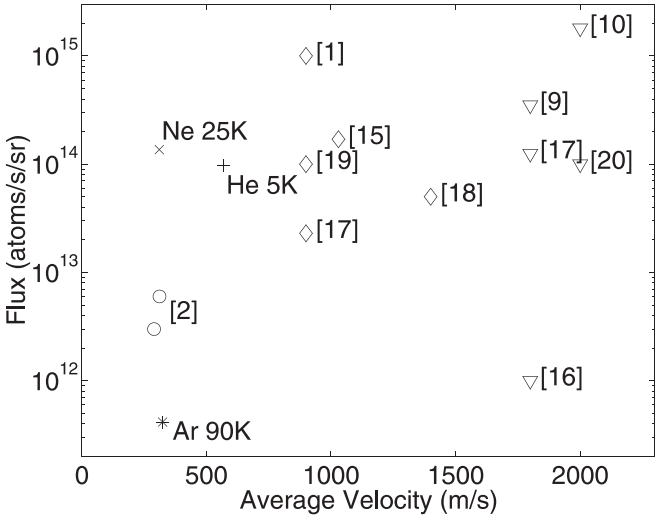

FIGURE 8 Flux and velocity for metastable gas sources: for the new source three metastable species (cold-finger temperature): helium (5 K) (+); neon (25 K); (×); argon (90 K) (∗); other referenced sources at 300 K (▽), 77 K (◇) and ∼5 K(○). Numbers give citations for the data

condensation point. Figure 8 shows the source flux and velocity obtained using He (5 K), Ne (25 K) and Ar (90 K) at optimum flux conditions. Although the α values for He ($\sim 200, 5$ K), Ne ($\sim 150, 25$ K) and Ar ($\sim 260, 90$ K) are similar at these source temperatures, the average velocity for He is found to be considerably higher. The flux for Ar is also notably lower under these operating conditions, which may be due to cluster formation.

5 Conclusion

We have developed a new source for metastable rare gas atoms based on a liquid-He cooled hollow cathode discharge. This source generates fluxes exceeding 10^{14} atoms/ster/s, which is an order of magnitude lower than our previous liquid-N_2 cooled source [1] but with considerably lower average velocities (450–700 m/s). The optimized source configuration comprises an external anode placed in the collision-free region downstream from a 1.0 mm diameter nozzle in a boron nitride cap, located at the end of a cylindrical hollow copper cathode. The source has also been shown to yield similarly high fluxes of metastable Ne (and to a lesser extent, Ar) at average velocities ~ 300 m/s.

By comparison, the liquid-He cooled source described in [2] yields a flux of $< 10^{13}$ atoms/ster/s at average velocities ~ 300 m/s. The somewhat higher average velocity for our source is offset by almost two orders of magnitude increase in flux. Future experiments will investigate the efficiency of this high flux, liquid-He cooled design as a source for loading a metastable helium beam line and a magneto-optic trap.

ACKNOWLEDGEMENTS We would like to acknowledge the expert technical assistance of I. McRae, C. MacCleod and S. Battisson in the design and manufacture of the source. J. Swansson would like to acknowledge the scholarship support of the ANU, and K. Baldwin and A. Truscott the financial support of the Australian Research Council for the Centre of Excellence for Quantum-Atom Optics.

REFERENCES

1 W. Lu, M.D. Hoogerland, D. Milic K.G. H Baldwin, S.J. Buckman: Rev. Sci. Instrum. **72**, 2558 (2001)
2 G.R. Woestenenk, J.W. Thomsen, M. Rijnbach, P. van der Straten, A. Niehaus: Rev. Sci. Instrum. **72**, 3842 (2001)
3 A. Robert, O. Sirjean, A. Browaeys, J. Poupard, S. Nowak, D. Boiron, C.I. Westbrook, A. Aspect: Science **292**, 46 (2001); F. Pereira Dos Santos, J. Léonard, J. Wang, C.J. Barrelet, F. Perales, E. Rasel, C.S. Unnikrishnan, M. Leduc, C. Cohen-Tannoudji: Phys. Rev. Lett. **86**, 3459 (2001)
4 H.J. Metcalf, P. van der Straten: *Laser Cooling and Trapping* (Springer, New York 1999)
5 D. Milic, M.D. Hoogerland, K.G.H. Baldwin, S.J. Buckman: Appl. Opt. **40**, 1907 (2001)
6 W. Lu, K.G.H. Baldwin, M.D. Hoogerland, S.J. Buckman, T.J. Senden, T.E. Sheridan, R.W. Boswell: J. Vac. Sci., Technol. B **16**, 3846 (1998)
7 R.G. Dall, M.D. Hoogerland, D. Tierney, K.G.H. Baldwin, S.J. Buckman, Appl. Phys. B **74**, 11 (2002)
8 C.J. Dedman, K.G.H. Baldwin, M. Colla: Rev. Sci. Instrum. **72**, 4055 (2001)
9 D.W. Fahey, W.F. Parks, L.D. Schearer: J. Phys. E **13**, 381 (1980)
10 K. Ohno, T. Takami, K. Mitsuke, T. Ishida: J. Chem. Phys. **94**, 2675 (1991)
11 J. Kawanaka, M. Hagiuda, K. Shimizu, F. Shimizu, H. Takuma: Appl. Phys. B **56**, 21 (1993)
12 K.G.H. Baldwin, R.P. Swift, R.O. Watts: Rev. Sci. Instrum. **58**, 812 (1987)
13 N.F. Ramsey In *Atomic, Molecular, and Optical Physics Atoms and Molecules*, F.B. Dunning, R.G. Hulet (Eds.) (Academic Press, 1996)
14 M.D. Morse In *Atomic, Molecular, and Optical Physics Atoms and Molecules*, F.B. Dunning, R.G. Hulet (Eds.) (Academic Press, 1996)
15 W. Rooijakkers, W. Hogervorst, W. Vassen: Opt. Comm. **135**, 149 (1997)
16 N. Vansteenkiste, C. Gerz, R. Kaiser, L. Hollberg, C. Salomon, A. Aspect: J. Phys. II France **1**, 1407 (1991)
17 O. Carnal, M. Sigel, T. Sleator, H. Takuma, J. Mlynek: Phys. Rev. Lett. **67**, 3231 (1991)
18 M. Doery, M. Widmer, J. Bellanca, E. Vredenbrecht, T. Bergeman, H. Metcalf: Phys. Rev. Lett. **72**, 2546 (1994)
Opt.
19 H.C. Mastwijk, M. van Rijnbach, J.W. Thomsen, P. Van der Straten, A. Niehaus: Eur. Phys. J. D **4**, 131 (1998)
20 M. DeKieviet, M. Dürr, S. Epp, F. Lang, M. Theis: Rev. Sci. Instrum. **75**, 345 (2004)